Combined Effects of Conjugation Pattern and Alkoxy Side Chains on the Photovoltaic Properties of Thiophene-Containing PPE-PPVs

DANIEL AYUK MBI EGBE,[1] LE HUONG NGUYEN,[2] KATHY SCHMIDTKE,[1] ANDREAS WILD,[1] CHRISTOPH SIEBER,[3] SERAP GUENES,[2] NIYAZI SERDAR SARICIFTCI[2]

[1]Institut für Organische Chemie und Makromolekulare Chemie der Friedrich-Schiller Universität, Humboldtstr. 10,07743 Jena, Germany

[2]Linz Institute for Organic Solar Cells (LIOS), Johannes Kepler University Linz, Altenbergerstr. 69, A-4040 Linz, Austria

[3]Max-Planck-Institut für Polymerforschung, Ackermannweg 10, D-55128 Mainz, Germany

Received 23 October 2006; accepted 7 December 2006
DOI: 10.1002/pola.21928
Published online in Wiley InterScience (www.interscience.wiley.com).

ABSTRACT: This contribution presents the synthesis and properties of four thiophene-containing poly(-*p*-arylene-ethynylene)/poly(-*p*-arylene-vinylene)s, **PIa-b** and **PIIa-b**, whose repeating units (RU) consist either of 1:2 or 2:2 *triple bond*/*double bond* ratio, and which bear *linear* alkoxy side chains not longer than octyloxy and *branched* 2-ethylhexyloxy. **PIa-b** and **PIIa-b** exhibit similar absorption and emission behaviour in dilute solution (λ_a = 483–486 nm, λ_e = 540 nm) as well as in solid state (λ_a = 500, 530 nm, λ_e = 560 nm), whereby slightly higher fluorescence quantum yields (Φ_f) were obtained for **PI** than for **PII** systems, as a result of higher number of thiophene units within the RU of **PII**. An enhancement of the Φ_f-value from 0% to 3% is obtained after replacing *linear* octadecyloxy in **PIIc-e** by *bulky branched* 2-ethylhexyloxy in **PIIa-b**. Nonoptimized solar cells of configuration ITO/PEDOT:PSS/polymer: PCBM (1:3 weight ratio)/LiF/Al show open circuit voltages as high as 900 mV for **PIa-b** and 800 mV for **PIIa-b**. Reducing the size of the side chain from R = 2-*ethylhexyl* in **PIa** to R = *methyl* in **PIb** leads to a significant increase of the short circuit current, I_{SC}, from ca. 2.5 mA to ca. 3.7 mA and consequently to an enhancement of the energy conversion efficiency, $\eta_{AM1.5}$, from ca. 1.2% to ca. 1.7%. This is due to an extended donor-acceptor interfacial area, as evidenced by AFM topology pictures showing smaller nanoscale clusters size in **PIb** than in **PIa** active layer. The same change led to minimal effect in **PII** systems. © 2007 Wiley Periodicals, Inc. J Polym Sci Part A: Polym Chem 45: 1619–1631, 2007

Keywords: Atomic force microscopy; conjugated polymers; cooperative effects; photophysics; synthesis

INTRODUCTION

Thiophene-containing oligomeric[1,2] and polymeric[3,4] compounds have been at the focus of extensive research in recent years, due to their promising applications in electrochromic devices,[5]

Correspondence to: D. Ayuk Mbi Egbe (E-mail: c5ayda@unijena.de)

Journal of Polymer Science: Part A: Polymer Chemistry, Vol. 45, 1619–1631 (2007)

biosensors,[6] electrochemical supercapacitors,[7] anti-corrosion,[8] photodetectors,[9] light-emitting diodes,[10] organic field-effect transitors (OFETs)[2(d),11,12], and solar cells.[13] In the domain of OFETs using conjugated polymeric systems, for instance, high charge carrier mobilities have been so far achieved with regioregular head-to-tail arranged poly(3-hexylthiophene) (P3HT) ($\sim$0.1 to 0.2 cm^2/V s) and with liquid-crystalline poly{2,5-bis(3-alkylthiophene-2-yl)thieno[3,2-*b*]thiophene}(0.2–0.6 cm^2/V s).[12] These high values are attributed to high degree of intermolecular ordering, which is moreover a prerequisite to be fulfilled by the active layer of high performance organic photovoltaic devices. This explains the significant research focus laid on P3HT in the field of organic solar cells.[13(b)] Power conversion efficiencies, η, of up to 5% (under AM1.5 conditions) have been achieved recently by many research groups using P3HT.[14,15] η is directly proportional to the filling factor (FF), the open circuit voltage (V_{OC}) and the short circuit current (I_{SC}). Polythiophene-based cells generally exhibit high FF as well as high I_{SC}, but V_{OC}'s, which seldom exceed 0.65 V.[13(b)] However, solar cells made from poly(arylene-ethynylene)-*alt*-poly (arylene-vinylene) (PAE-PAV) are mostly characterized with higher V_{OC}'s.[16–18] V_{OC}-values of up to 0.94 V in polymer-PCBM (6,6-phenyl C_{61} butyric acid methylester) heterojunction systems and up to 1.50 V in polymer–polymer blend as well as bilayer systems have been achieved.[16–18] Comparatively lower I_{SC}'s have been observed with these systems.

Our research interest of recent has been to insert thiophene units within PPE-PPV backbones and to study the photovoltaic behavior of the resulting polymers. Such copolymers are expected to have optical band gap energies of $\sim$2.0 eV, due to the electron-rich thiophene moieties. Moreover, thiophene unit is known to induce planarity in polymeric backbone, which is related to the very small torsion angle that it forms with its neighbors.[19] This aspect is of great significance for enhanced intermolecular packing (π-stackings) and ordering, which is relevant for charge transport ability in the bulk and the resulting short circuit current I_{SC}. In this line we first synthesized polymers **PIa** (Chart 2) and **PIIc-e** (Chart 1) using the Horner–Wadsworth–Emmons coupling reaction of luminophoric dialdehydes and bisphonate esters.[18] **PIIc-e** were obtained as "oligomers" (P_n = 4–7), attributed to the low reactivity of the reacting species probably due to steric hindrances caused by the large octadecyloxy side chains, which were necessary for a good solubility of the compounds. Low molecular weight is one of the main reasons for the poor photovoltaic parameters obtained from **PIId** cells (best cell: V_{OC} = 500 mV, I_{SC} = 1.4 mA/cm^2, FF = 37%, $\eta_{AM1.5}$ = 0.3%) as compared to **PIa** (P_n = 34) cells (best cell: V_{OC} = 900 mV, I_{SC} = 2.5 mA/cm^2, FF = 54%, $\eta_{AM1.5}$ = 1.2%). This has been demonstrated by Scherf et al. using P3HT samples of different molecular-weights.[4(b)] Other important reasons, which are related to the longer octadecyloxy and dodecyloxy side groups, are the low amount of the active donor component per volume unit as well as the "insulating" nature of the long side groups hampering the movement of charges as well as hindering a good donor–acceptor contact.[16(d)]

In this article, our attention is directed on polymers **PIa-b** and **PIIa-b**, bearing linear side chains not longer than octyloxy and *branched* 2-ethylhexyloxy. Their higher molecular weights [P_n > 20, polydispersity index (PDI) <3] and Gauss-like molecular-weight distribution allow a comparison of their photophysical and photovoltaic properties while focusing on the concerted effects of the conjugation pattern and the grafted alkoxy side chains.

EXPERIMENTAL

Instrumentation

^{1}H NMR and ^{13}C NMR spectra were obtained in deuterated chloroform or benzene using either a Bruker DRX 400 or a Bruker AC 250. Chemical shifts (δ-values) are given in parts per million with tetramethylsilane as an internal standard. Elemental analysis was measured on a CHNS-932 Automat Leco. Infrared spectroscopy was recorded on a Nicolet Impact 400. A home-made apparatus served for the thermogravimetric measurements. Gel-permeation chromatography (GPC) was performed on a set of Knauer using THF as eluent and polystyrene as a standard. The absorption spectra were recorded in dilute chloroform or THF solution on a Perkin–Elmer UV/VIS-NIR Spectrometer Lambda 19. Quantum-corrected emission spectra were measured in dilute chloroform solution with a LS 50 luminescence spectrometer (Perkin–Elmer). The solution photoluminescence quantum yields were calculated according to Demas and Crosby against quinine sulfate in 0.1 N sulfuric acid as a standard (Φ_f = 55%).[20] Thin film absorption and emission spectra were measured with a Hitachi F-4500 Fluorescence Spectrophotometer. The films were spin-casted from chlorobenzene solution. The

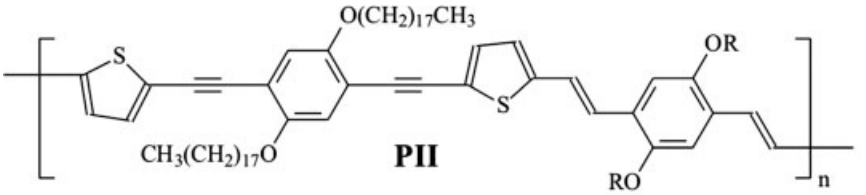

PIIc: R= octadecyl, M_n = 8,000, M_w = 19,700, M_w/M_n =2.4, P_n = 5
PIId: R = dodecyl, M_n = 9,000, M_w = 20,000, M_w/M_n = 2.2, P_n = 7
PIIe: R = octyl, M_n = 4,400, M_w = 13,000, M_w/M_n =2.9, P_n = 4

Chart 1. Chemical structures and data from GPC (THF, polystyrene as standard) of polymers **PIIc-e**.[18]

quantum yield in solid state was determined against a CF_3P-PPV (poly{1,4-phenylene-[1-(4-trifluoromethylphenyl)-vinylene]-2,5-dimethoxy-1,4-phenylene-[2-(4-trifluoromethylphenyl)-vinylene]}) copolymer reference whose quantum yield has been measured by integrating sphere to be 0.43.[21]

Electrochemical Investigation

The electrochemical behavior of **PIb** and **PIIa-b** was investigated by cyclic voltammetry, which was performed in a solution of Bu_4NClO_4 (98%, ~0.1 M) in anhydrous acetonitrile at a scan rate of 100 mV/s. A platinum electrode coated with a thin polymer film (casted from either THF or dichloromethane solution) was used as the working electrode. A platinum foil served as the counter electrode and Ag/AgCl electrode served as the reference electrode (RE).

After each measurement the RE was calibrated with ferrocene (E^0 = 400 mV versus NHE) and the potential was corrected to NHE according to the difference of E^0 (ferrocene) and the measured $E^{1/2}$(ferrocene).

Atomic Force Microscopy

Atomic force microscopy (AFM) studies were performed by using a Digital Instruments Dimension 3100 in the tapping mode. The AFM characterization was performed in an area of the active layer of the photovoltaic device where the electrode was not deposited.

Solar Cell Fabrication

Blend solutions of polymers **PIa-b** or **PIIa-b** as donor component and the C_{60}-derivative 1-(3-methoxycarbonyl) propyl-1-phenyl [6,6]C_{61} (PCBM) as acceptor at a weight ratio of 1:3 were prepared in chlorobenzene at a concentration of 10 mg polymer/mL. Poly(3,4-ethylenedioxythiophene):poly(styrenesulfonate) (PEDOT:PSS) (Baytron PH, Bayer Germany) was spin-coated on top of indium-tin oxide (ITO) (Merck, Germany) coated glass (~25 Ω/cm^2). Then the active layer (polymer: PCBM blend) was spin-coated on the annealed PEDOT:PSS layer (about 80 nm thick). Lithium fluoride (LiF, 6 Å) and 80 nm thick Al electrode was deposited on the blend film by thermal evaporation at $\sim 5 \times 10^{-6}$ mbar. All current–voltage (I-V) characteristics of the photovoltaic devices were measured using a Keithley SMU 2400 unit under inert atmosphere (argon) in a dry glove box. A Steuernagel solar simulator under AM 1.5 conditions was used as the excitation source with an input power of 100 MW/cm^2 white light illumination.

Materials

All starting materials were purchased from commercial suppliers (Fluka, Merck, and Aldrich). Toluene was dried and distilled over sodium and benzophenone. Diisopropylamine was dried over KOH. If not otherwise specified solvents or solution were degassed by bubbling with argon or nitrogen 1 h prior to use.

The syntheses of 1-(4-formyl-2,5-dioctyloxyphenyl)-2-(5-formylthiophene-2-yl)-acetylene (**1**),[18] 2,5-dialkoxy-*p*-xylylene-bis(diethylphosphonate) (**2**),[22] 1,4-diethynyl-2,5-bis(2-ethylhexyloxy)benzene (**3**),[22(a)] and poly{1,4-(2,5-dioctyl)]phenylene-ethynylene-thiophene-2,5-ylene-vinylene-1,4-[2,5-bis(2′-ethyl)hexyloxy]phenylene-vinylene} (**PIa**)[18] have been reported elsewhere.

1,4-Bis(2′-ethyl)hexyloxy-2,5-bis (5-formylthiophene-2-yl-ethynyl)benzene (5)

To a degassed solution of 1,4-bis(2′-ethylhexyl)oxy-2,5-diethynylbenzene (**3**) (5.6 g, 14.31 mmol) in 150 mL toluene and 100 mL diisopropylamine were added $Pd(PPh_3)_4$ (673 mg, 0.57 mmol, 4 mol %), CuI (118 mg, 0.57 mmol, 4 mol %), and 5-bromo-2-thiophenecarbaldehyde (3.58 mL, 28.62 mmol). The mixture was stirred at 70 °C for 24 h. After filtration of the precipitated ammonium bromide salt, the solvent was removed under reduced pressure. The residue was chromatographed on silica gel 60 column using toluene/hexane: 2/1 as eluent. The expected product was detected on TLC at $R_f = 0.7$ and was obtained as yellow powder.

Yield: 6.1 g (71%). ^{1}H NMR (250 MHz, $CDCl_3$): δ/ppm 0.89 (12H, m, CH_3); 1.26, 1.45 (16H, m, CH_2); 1.71 (2H, m, CH); 3.81 (4H, m, CH_2O); 6.92 (2H, s, phenylene H's); 7.22 (2H, d, $^3J = 5$ Hz, thiophene H) 7.60 (4H, d, $^3J = 5$ Hz, thiophene H), 9.79 (2H, s, CHO). ^{13}C NMR (62 MHz, $CDCl_3$): δ/ppm 11.29 (*C*H_3 ethyl); 14.05 (*C*H_3 hexyl); 23.03, 24.06, 29.10, 30.65 (*C*H_2), 39.53 (*C*H); 71.92 (*C*H_2O); 87.74, 94.64 (*C*≡*C*); 113.57, 116.02 (C_{phenyl}); 132.34, 132.89, 136.05, 144.00 ($C_{thiophene}$); 154.01 (C_{phenyl}-OR); 182.30 (*C*HO). IR (KBr): 2956 (m, ν_{as} CH_3); 2927 (s, ν_{as} CH_2); 2855 (m, ν_s CH_2); 2199 (w, ν C≡C); 1654 (s, $\nu_{aldehyde}$); 1217 (versus, $\nu_{Caryl\text{-}OR}$); 804 (s, $\gamma_{CH,}$ phenyl) cm^{-1}. UV–vis ($CHCl_3$) (λ_{max} (ε in L/mol cm)): 271 (12,000), 350(29,500), 421 (43,700). ANAL. calcd. for $C_{36}H_{42}O_4S_2$ (602.85): C, 71.72; H, 7.02; S, 10.64. Found: C, 71.62; H, 7.15; S, 10.38.

Poly{1,4-(2,5-dioctyl)]phenylene-ethynylene-thiophene-2,5-ylene-vinylene-1,4-[2-(2′-ethyl)hexyloxy-5-methyloxy]-phenylene-vinylene } (PIb)

Dialdehyde **1** (889 mg, 1.79 mmol) and 2-(2′-ethylhexyloxy)-5-methoxy-*p*-xylylene-bis(diethylphosphonate) (960 mg, 1.79 mmol) were dissolved in toluene (30 mL) while stirring vigorously under argon and heating under reflux. Potassium *tert*-butoxide (603 mg, 5.4 mmol) was added in portions to this solution; and the reaction mixture was heated at reflux for 3 h. After this time more toluene (50 mL) was added and the reaction was quenched with 10% aqueous HCl solution (25 mL). The organic phase was separated and extracted several times with distilled water until the water phase became neutral (pH = 6–7). The organic layer was dried with a Dean-Stark apparatus. The resulting toluene suspension was filtered and evaporated under reduced pressure to 30 mL and was precipitated in 700 mL methanol. After extraction in diethyl ether and drying under vacuum, 517 mg of dark red substance were obtained.

Yield: 40%. GPC (THF): $M_w = 41{,}900$ g/mol, $M_n = 14{,}500$ g/mol, $M_z = 77{,}100$ g/mol, polydispersity index (PDI) = 2.89. ^{1}H NMR (400 MHz, $CDCl_3$): δ/ppm 0.91→1.59 (57H, m, CH_3's and CH_2's); 1.90 (1H, s, CH); 3.68 (3H, s, CH_3O); 3.96 → 4.12 (6H, m, CH_2O); 6.85 → 7.53 (10H, m, vinylene and arylene H's). ^{13}C NMR (100 MHz, $CDCl_3$): δ/ppm 11.37 (*C*H_3 ethyl); 14.09 (*C*H_3 hexyl); 22.68, 23.13, 24.32, 26.18, 29.35, 29.44, 30.91, 30.99, 31.87 (*C*H_2), 39.82 (*C*H); 56.27 (OCH_3); 69.42, 69.75, 70.07, 71.75 (*C*H_2O); 88.04, 90.34 91.65 (*C*≡*C*); 113.57, 116.02, 108.88, 109.22, 110.43, 111.10, 112.44, 116.71, 121.86 124.13, 127.05, 127.35, 128.85, 131.15, 132.41, 145.29 (arylene and vinylene C's); 150.48, 150.68, 151.52, 154.17 (C_{aryl}-OR). IR (KBr): 3037 (w, ν_{CH}); 2953 (m, ν_{as} CH_3); 2923 (s, ν_{as} CH_2); 2854 (m, ν_s CH_2); 1495 (m, $\nu_{C=C}$); 1202 (s, $\nu_{Caryl\text{-}OR}$), 1036 (m, $\nu_{C=S}$); 967 (s, $\nu_{CH=CH}$ trans) cm^{-1}. UV–vis (THF) (λ_{max} (ε in L/mol cm)): 344 (12,300), 482 (60,300). ANAL. calcd. for $(C_{47}H_{64}O_4S)_n$ $(725.07)_n$: C, 77.85; H, 8.90; S, 4,42. Found: C, 76.52; H, 8.50; S, 4.18.

Poly[2,5-thiophene-ylene-ethynylene-1,4-(2,5-bis(2′-ethylhexyloxyphenylene)-ethynylene-2,5-thiophene-ylene-vinylene-1,4-(2,5-bis(2′-ethylhexyloxyphenylene)-vinylene] (PIIa)

Dialdehyde **5** (1 g, 1.66 mmol) and 2,5-bis(2′-ethylhexyloxy)-*p*-xylylene-bis(diethylphosphonate) (1.053 g, 1.66 mmol) were given to 20 mL toluene and the mixture was heated to reflux. After portionwise addition of potassium *tert*-butoxide (558 mg, 5 mmol), it was refluxed for 3 h. The quenching of the reaction and the work up were similar as described earlier. Dark red compound (917 mg, 58%) was obtained. GPC (THF): $M_w = 99{,}400$ g/mol, $M_n = 35{,}200$ g/mol, $M_z = 32{,}000$ g/mol, PDI = 2.81.

^{1}H NMR (250 MHz, $CDCl_3$): δ/ppm 0.96 → 1.58 (60H, bm, CH_3 and CH_2); 1.85 (4H, b, CH); 3.98 (8H, b, CH_2O); 7.02 → 7.30 (10H, bm, arylene and vinylene H's). ^{13}C NMR (100 MHz, $CDCl_3$): δ/ppm 11.35 (*C*H_3 ethyl); 14.12 (*C*H_3 hexyl); 23.11, 24.15, 24.34, 29.21, 29.29, 30.73, 30.97 (*C*H_2), 39.66, 39.82 (*C*H); 71.67, 72.12 (*C*H_2O); 88.93, 91.26 (*C*≡*C*); 110.21, 113.82, 116.13, 121.82, 122.02 (C_{phenyl}); 124.30, 132.63 (*C*=*C*); 125.92, 126.42, 131.69 ($C_{thiophene}$); 145.68, 151.33, 153.79 (C_{phenyl}-OR). IR (KBr): 3039 (w, ν_{CH}); 2957 (m, ν_{as} CH_3);

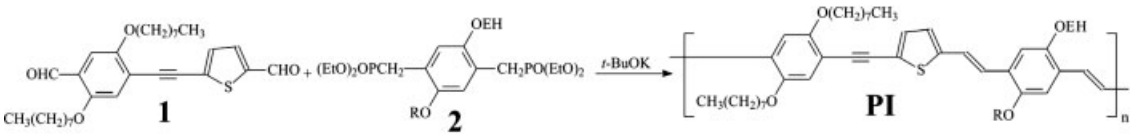

EH = 2-ethylhexyl

PIa: R = 2-ethylhexyl, M_n = 28,000, M_w = 74,000, M_w/M_n = 2.6, P_n = 34
PIb: R= methyl, M_n = 14,500, M_w = 42,000, M_w/M_n = 2.8, P_n = 20

Chart 2. Synthesis of polymers **PIa** and **PIb** and data from GPC (THF, polystyrene as standard).

2923 (s, ν_{as} CH_2); 2857 (m, ν_s CH_2); 2194 (w, $\nu_{C\equiv C}$); 1493 (m, $\nu_{C=C}$); 1210 (s, $\nu_{Caryl\text{-}OR}$); 1028 (m, $\nu_{C=S}$); 949 (s, $\gamma_{CH=CH}$ trans) cm^{-1}. UV–vis ($CHCl_3$) (λ_{max} (ε in L/mol cm)): 486 (19,500). ANAL. calcd. for $(C_{60}H_{80}O_4S_2)_n$ $(929.4)_n$: C, 77.55; H, 8.68; S, 6.90. Found: C, 74.51; H, 8.30; S, 6.89.

Poly{2,5-thiophene-ylene-ethynylene-1, 4-[2,5-bis(2′-ethyl)hexyloxyphenylene]-ethynylene-2,5-thiophene-ylene-vinylene-1,4-[2-(2′-ethyl) hexyloxy-5-methoxyphenylene]-vinylene} (PIIb)

Dialdehyde **5** (1 g, 1.66 mmol) and 2-(2′-ethylhexyloxy)-5-methoxy-*p*-xylylene-bis(diethylphosphonate) (0.891 g, 1.66 mmol) were given in 30 mL toluene and the mixture was heated to reflux. After portionwise addition of potassium *tert*-butoxide (558 mg, 5 mmol), it was refluxed for 3 h. The reaction was quenched after addition of 80 mL toluene and 100 mL HCl solution (10%). The work up was done in a similar way as described above. Dark red polymer (494 mg, 36%) was obtained after 25 h extraction with diethyl ether of the crude product. GPC (THF): M_w = 130,000 g/mol, M_n = 46,000 g/mol, M_z = 420,000 g/mol, PDI = 2.81.

^{1}H NMR (400 MHz, C_6D_6): δ/ppm 1.05 → 1.80 (38H, m, CH_3 and CH_2); 3.47 (3H, s, CH_3O); 3.70 and 3.85 (6H, br, CH_2O); 6.84→7.80 (12H, m, vinylene and arylene H's). ^{13}C NMR (100 MHz, C_6D_6): δ/ppm 11.58 (*C*H_3 ethyl); 14.35 (*C*H_3 hexyl); 23.52, 24.51, 24.58, 24.75, 29.57, 31.18, 31.40 (*C*H_2); 40.01, 40.18 (*C*H); 55.65 (*C*H_3O); 71.69 (*C*H_2O); 89.54, 92.50 (*C*≡*C*); 109.59, 110.98, 114.41, 116.43, 122.41, 122.95, 133.00 (C_{aryl}'s); 125.02, 126.53 (*C*=*C*); 145,98, 151,98, 154,43 (C_{aryl}-OR). IR (KBr): 3038 (w, ν_{CH}); 2956 (m, ν_{as} CH_3); 2924 (s, ν_{as} CH_2); 2857 (m, ν_s CH_2); 2190 (w, $\nu_{C\equiv C}$); 1492 (m, $\nu_{C=C}$}); 1205 (versus, $\nu_{Caryl\text{-}OR}$); 1032 (m, $\nu_{C=S}$); 947 (s, $\gamma_{CH=CH}$ trans) cm^{-1}. UV–vis (λ_{max} (ε in L/mol cm), THF): 481 (66,000). ANAL. calcd. for $(C_{60}H_{80}O_4S_2)_n$ $(929.4)_n$: C, 77.55; H, 8.68; S, 6.90. Found: C, 74.51; H, 8.30; S, 6.89.

RESULTS AND DISCUSSION

Synthesis and Structural Characterization

Charts 2 and 3 illustrate the synthetic path to polymers **PIa-b** and **PIIa-b**, respectively. The polymers were prepared through HWE coupling reactions of 2,5-dialkoxy-*p*-xylylene-bis(diethylphosphonate) (**2**)[22] with either 1-(4-formyl-2,5-dioctyloxyphenyl)-2-(5-formylthiophene-2-yl)-acetylene (**1**),[18] (for **PIa-b**) or 1,4-bis(2′-ethyl)hexyloxy-2,5-bis(5-formylthiophene-2-yl-ethynyl)benzene (**5**) [obtained from the Sonogashira-Hagihara cross-coupling reaction[23] of 1,4-diethynyl-2,5-bis(2-ethylhexyloxy)benzene (**3**)[22(a)] with the commercially available 5-bromo-thiophene-2-carboxaldehyde (**4**) as a yellow substance in 71% yield] (for **PIIa-b**) under similar reaction conditions as described elsewhere.[18] To achieve good solubility of polymers **PIIa-b**, it was essential to graft branched 2-ethylhexyloxy side chains on **5** instead of linear octyloxy as in **1**. Stronger intermolecular π-π-stackings are structurally expected from **PII**-type polymers (consisting of two triple bonds and two thiophene units within their repeating units (RU)) than in **PI**-type compounds. Such strong intermolecular interactions impede the solubility of conjugated systems. Using diethyl ether as extraction medium of the crude polymeric end products proved to be crucial for an easy access to high molecular-weight polymer fractions exhibiting a Gauss-like molecular-weight distribution and Flory-like polydispersity indexes about 2. $P_n \approx$ 20–56 were estimated for the four polymers.

The chemical structures of dialdehyde **5** and polymers **PIb** and **PIIa-b** were confirmed by ^{1}H and ^{13}C NMR, elemental analysis, and infrared spectroscopy. Figures 1–3 depict the ^{13}C NMR

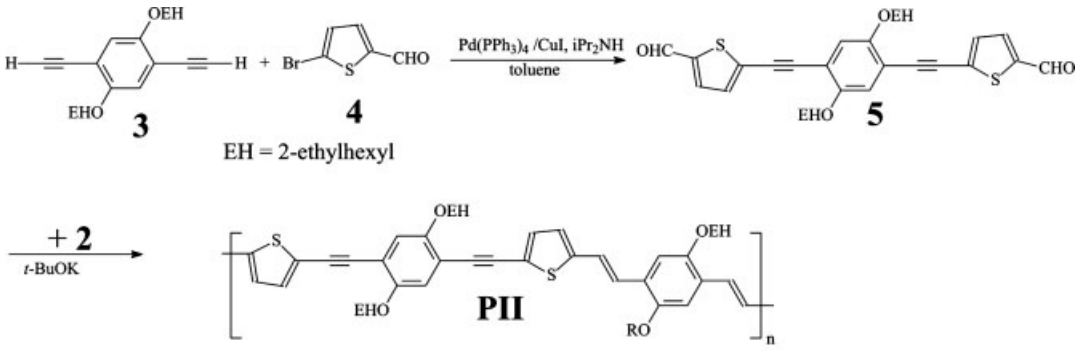

PIIa: R= 2-ethylhexyl, M_n = 35,000, M_w = 99,400, M_w/M_n = 2.8, P_n = 38
PIIb: R = methyl, M_n = 46,000, M_w = 130,000, M_w/M_n = 2.8, P_n = 56

Chart 3. Synthesis of polymers **PIIa** and **PIIb** and data from GPC (THF, polystyrene as standard).

spectra of **PIb**, **5**, and **PIIa**, respectively, in deuterated chloroform. The various peaks could be readily assigned to the corresponding carbons atoms. The multiplicity of peaks in the ^{13}C NMR spectrum of **PIb** is a clear indication of non regioregularity in **PI** systems. Thermogravimetric analysis carried out at a heating rate of 10 K/min show high thermal stability for all polymers. The start of thermal degradation was detected about 300–350 °C, where approximately 5% weight-loss was recorded.

Photophysical Studies

As expected all four polymers are photoconductive in the absence of a sensitizer. Intrinsic photo-

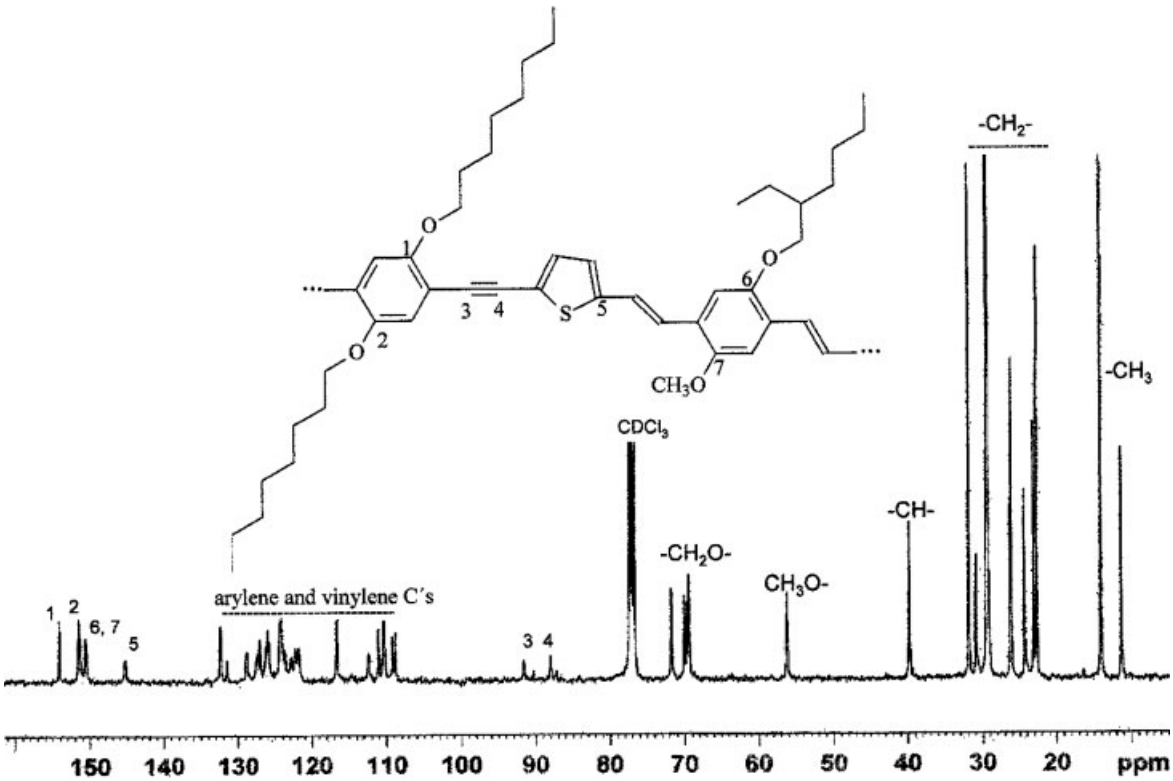

Figure 1. ^{13}C NMR spectrum (100 MHz, $CDCl_3$) of polymer **PIb**.

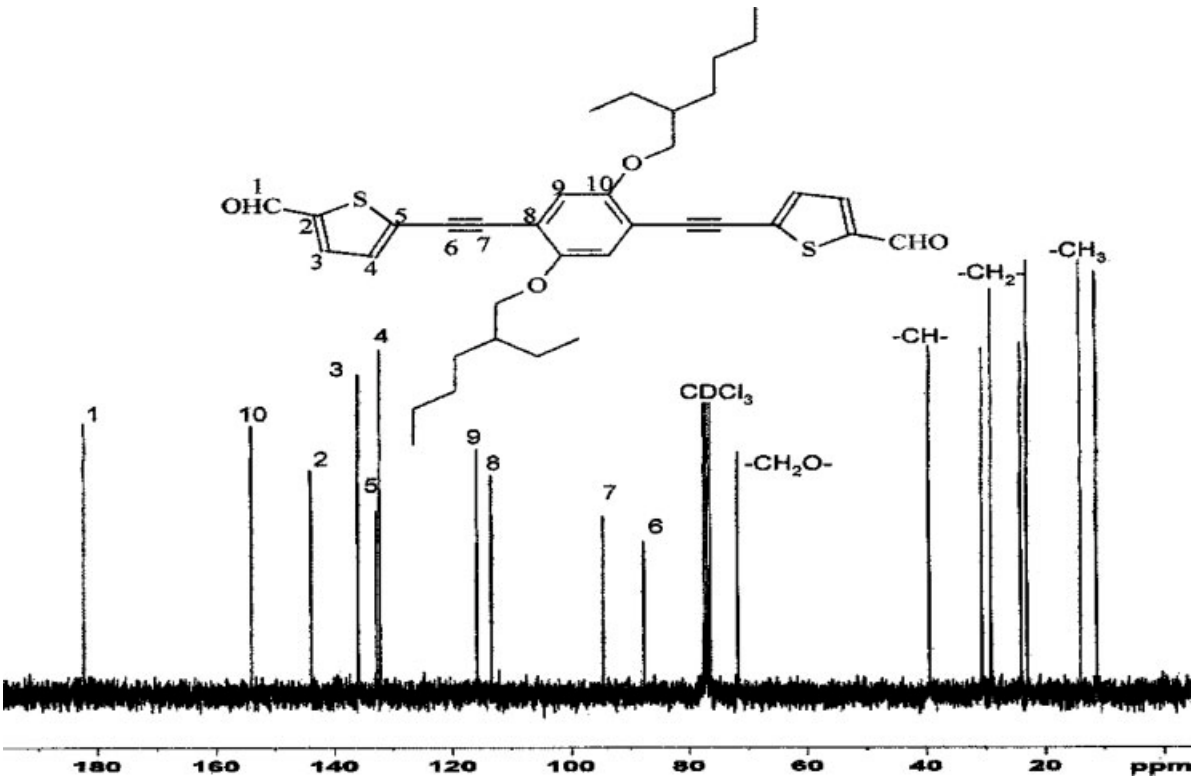

Figure 2. ^{13}C NMR spectrum (62 MHz, $CDCl_3$) of dialdehyde **5**.

conductivity was measured using the direct current technique at wavelengths between 1000 and 286 nm on thin film samples (thickness ~100 nm) casted from chlorobenzene solution, which were deposited on a slit having a width of 0.2 mm and a length of 10 mm. Maximal photocurrents, I_{ph}

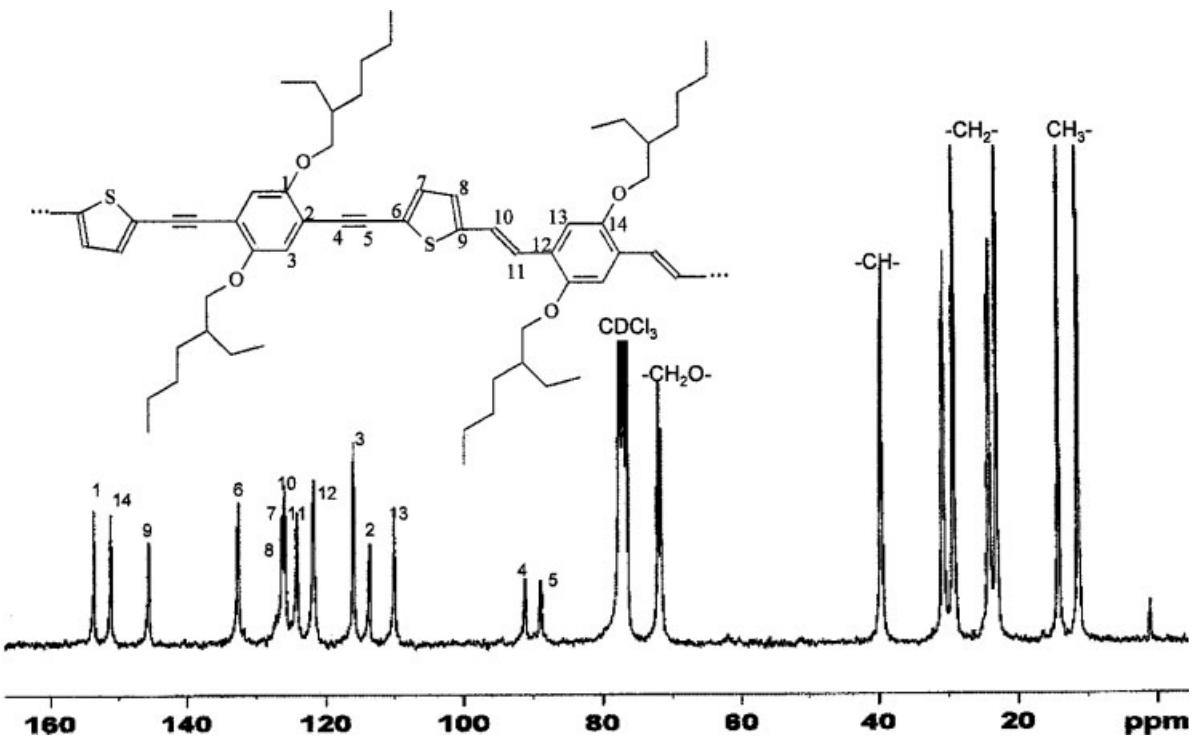

Figure 3. ^{13}C NMR spectrum (100 MHz, $CDCl_3$) of polymer **PIIa**.

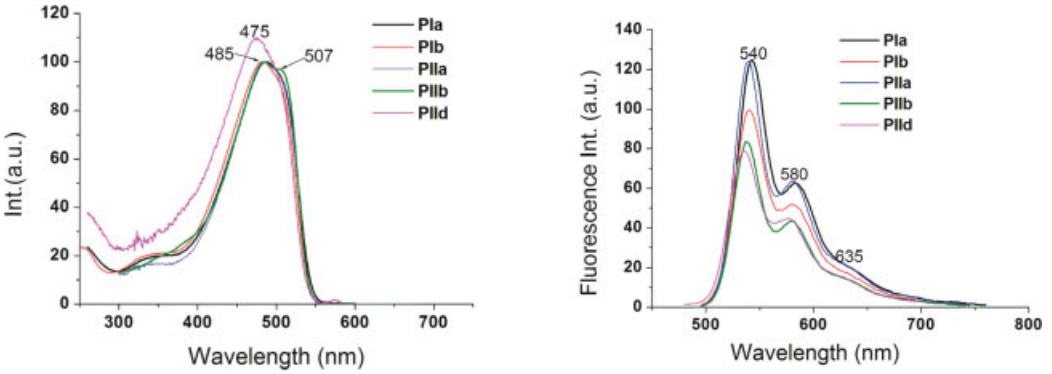

Figure 4. Normalized absorption spectra and fluorescence spectra of **PI** and **PII** systems in dilute chloroform solution.

(difference between total current in the presence of light and the dark current), of the order 10^{-11} Å between 18,000 and 19,000 cm^{-1} were obtained at a threshold voltage of 20 V.

Despite the difference in conjugation pattern both types of polymeric systems **PIa-b** and **PIIa-b** exhibit identical absorptive and emissive behavior in dilute chloroform solution as well as in thin film. This is ascribed to the similar lower energy phenylene–vinylene segment in both types of polymers, which has been proven to dictate the photophysical behavior of PPE-PPV systems.[24] Figures 4 and 5 depict the absorption and emission spectra in solution and in solid film, respectively. The optical data are summarized in Table 1. The main solution absorption bands consist of a peak about λ_a = 483–486 nm and a shoulder about 502–504 nm, which is significant in **PIIb**, but discrete in the other three polymers. Solution optical band gap energy, E_g^{opt25}, about 2.29 eV and extinction coefficients between 20,000 and 60,000 M^{-1}/cm were estimated. Solution emission spectra are characterized by a hyperchromic $S_{10} \rightarrow S_{00}$ transition about $\lambda_e = 540$ nm, a $S_{10} \rightarrow S_{01}$ transition about $\lambda_e = 580$ nm, and a $S_{10} \rightarrow S_{02}$ transition appearing as a shoulder peak about 635 nm, leading to a Stokes shift of ~2100 cm^{-1}. The low P_n polymers **PIIc-e**, in constrast, are characterized with a ~10 nm blue shift of the absorption and a ~5 nm of the emission relative to their higher P_n counterparts.[18(a)] Fluorescence quantum yields, Φ_f, between 25 and 50% were evaluated. The present Φ_f-values are at least 20% lower than those of solely phenylene-containing PPE-PPV systems,[25] due to inner heavy-atom effects assigned to the presence of sulfur atoms.[18] Enhanced planarity in thin films results in a ~20 nm bathochromic shift of thin film absorption and emission spectra relative to dilute solution. The splitting of the main absorption band suggests the formation of **H**- ($\lambda_a \approx 500$ nm) and **J**- ($\lambda_a \approx 530$ nm) aggregates, respectively.[26] The shape of the solution absorption band of **PIIb**, for instance, might be an indication of such aggregates formation already in the solution. Thin film E_g^{opt} value about 2.07 eV was estimated. The thin

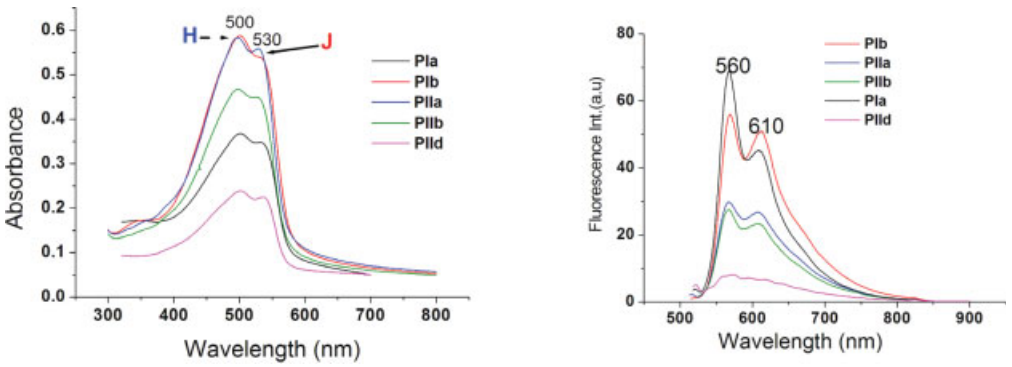

Figure 5. Thin film absorption and emission spectra of **PI** and **PII** systems. [Color figure can be viewed in the online issue, which is available at www.interscience.wiley.com.]

Table 1. Optical Data of Polymers **PIa-b** and **PIIa-b,d** in Dilute Chloroform and in Thin Solid Film Casted from Chlorobenzene Solution (Thickness ~ 100–150 nm)

Code	λ_a (nm)[a]	E_g^{opt} (eV)	λ_e (nm)	Stokes Shift (nm/cm)	Φ_f (%)
PIa	486	2.27	*542*, 583	56 (2100)	46
PIb	483	2.29	*540*, 579	57 (2200)	45
PIIa	486	2.29	*540*, 579	54 (2100)	36
PIIb	484, sh 504	2.29	*538*, 580	54 (2100)	25
PIId	475	2.31	*535*, 576	60 (2400)	51
PIa[b]	501, 531	2.06	*568*, 608	67 (2300)	7
PIb[b]	*500*, 538	2.07	*569*, 611	69 (2400)	5
PIIa[b]	*497*, 529	2.07	*560*, 610	69 (2400)	3
PIIb[b]	*498*, 526	2.07	*566*, 609	68 (2400)	3
PIId[b]	*501*, 535	2.10	–	–	~0

[a] Italic value corresponds to the maximum of the hyperchromic peak.
[b] Thin film.

film emission spectra are similarly well-structured as their corresponding solution spectra. $S_{10} \rightarrow S_{00}$ and $S_{10} \rightarrow S_{01}$ transitions are centered about $\lambda_e \approx 560$ nm and $\lambda_e \approx 610$ nm, respectively. Stokes shifts of approximately 2400 cm^{-1} were obtained. A significant increase of the fluorescence quantum yield from 0 to 3% is realized, when *linear* alkoxy side chains in **PIIc-e** are replaced by *branched* 2-ethylhexyloxy in **PIIa-b**; such branched side groups hinder very strong π-π interactions, which are known to contribute in the quenching of fluorescence. The supposedly predominance of **H**-aggregates, i.e., higher intensity of the higher energy peak at about 500 nm (Fig. 5, left), might be one of the major reasons of the generally low Φ_f-values (<10%) of these thiophene-containing systems.[27]

Electrochemical Studies

Figure 6 illustrates the CV curves of **PIb** and **PIIa-b**; the electrochemical data are summarized in Table 2. All potential values shown are versus normal hydrogen electrode (NHE). NHE-level in the Fermi scale used for HOMO-LUMO calculation was −4.75 eV.[28]

Nonreversible *p*-doping and reversible *n*-doping processes were observed for all polymers. Similar LUMO-levels about −3.14 eV and similar HOMO-levels about −5.43 eV were evaluated for both systems.[18(a)] However, the oxidation peak of **PII** systems was observed at higher potentials; this can be ascribed to the presence of higher number of the triple bonds in their RU.[29] As expected higher electrochemical band gap energies, $E_g^{ec} \approx 2.30$ eV, than optical band gap energies, $E_g^{opt} \approx 2.07$ eV, were obtained, suggesting side chains shielding effects as well as differences in polymer backbone conformation during the optical and electrochemical studies.[17(a),30]

Photovoltaic Studies

Nonoptimized solar cells of set up ITO/PEDOT:PSS/polymer:PCBM (1:3 weight ratio)/LiF/Al were designed using **PIa-b** and **PIIa-b**. The corresponding I-V curves are shown in Figure 7. Photovoltaic parameters of two cells from each polymer are given in Table 3. Cells

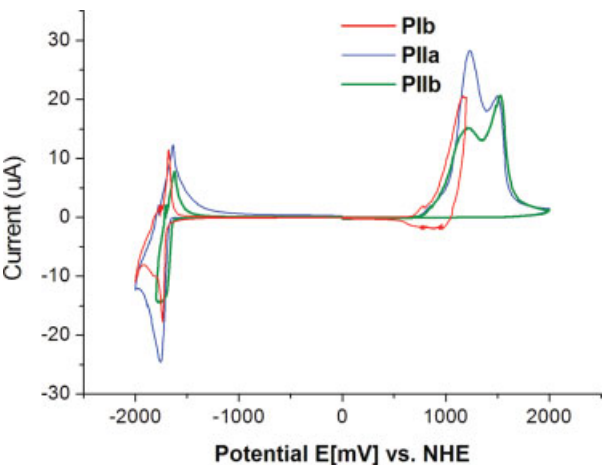

Figure 6. CV-curves of **PIb** and **PIIa-b**. [Color figure can be viewed in the online issue, which is available at www.interscience.wiley.com.]

Table 2. Electrochemical Data of the **PIa-b** and **PIIa-b**

Code	E^{ox}_{onset} (mV)	E^{red}_{onset} (mV)	E^{ox}_{peak} (mV)	E^{red}_{peak} (mV)	HOMO (eV)	LUMO (eV)	E^{ec}_{g} (eV)
PIa	+680	−1610	+890	−1780	−5.43	−3.14	2.29
PIb	+680	−1610	+1170	−1730	−5.43	−3.14	2.28
PIIa	+700	−1610	+1230, +1500	−1760	−5.45	−3.14	2.31
PIIb	+700	−1610	+1215, +1540	−1760	−5.45	3.14	2.31

HOMO and LUMO levels were estimated using following equation: HOMO/LUMO = $(-E_{onset} - 4.75)$ eV.[27]

from both **PIa** and **PIb** have similar open circuit voltage, V_{OC} = 900 mV, as well as similar FF = 50–54%, but different short circuit currents, I_{SC}, and consequently different energy conversion efficiencies, $\eta_{AM1.5}$. By reducing the bulkiness and length of the side chain from R = 2-*ethylhexyl* in **PIa** to R = *methyl* in **PIb**, a significant increase of I_{SC} from ∼2.5 to ∼3.7 mA is obtained, leading to an enhancement of $\eta_{AM1.5}$ from ∼1.2 to ∼1.7%. This is due to a larger donor–acceptor interfacial area in **PIb** than in **PIa** cells, as evidenced by the smaller nanoscale clusters size observed in the AFM topology picture of **PIb** than in **PIa** active layer (Fig. 8). Large interfacial area between donor and acceptor phases provides sufficient charge separation in the case of **PIb**. In general, optimal morphology control requires the interfacial area between donor and acceptor to be maximized in a trade-off with improved percolation through the film avoiding charge carrier recombination losses. Tuning the side chain length of the polymer in this work contributed to the morphology control that is one of key issues to enhance the efficiency. Carrying out the same change of side groups from **PIIa** to **PIIb** results in a minimal increase of I_{SC} from ca 4.2 to ∼4.5 mA, so that cells from both polymers exhibit similar photovoltaic parameters (Table 3); similar $\eta_{AM1.5}$-value of approximately 1.50% was obtained in this case.

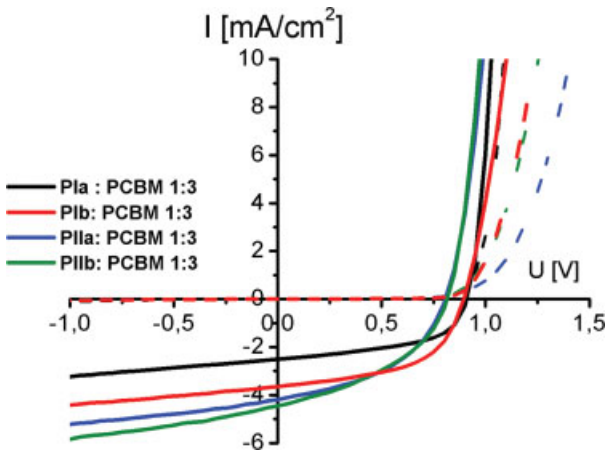

Figure 7. Current–voltage (I-V) curves of **PIa-b** and **PIIa-b** solar cells in dark (dashed line) and under illumination (solid line) with white light at irradiation intensity of 100 mW/cm^2. [Color figure can be viewed in the online issue, which is available at www.interscience.wiley.com.]

Figure 9 depicts the AFM pictures of the active layer of **PIIa-b**,**d** cells. There is no clear donor–acceptor phase separation of the active layer in **PIIa-b** cells, confirming their similar photovoltaic performance. This might be conditioned by the backbone structure-related regioregularity together with enhanced rigidity and coplanarity. However, very large phase separation arises, after attaching very long *dodecyloxy* and *octadecyloxy* side chains as in **PIId** [Fig. 9(a)]. This coarse phase separation may explain among other reasons for the poor PV performance as aforementioned.

The differences between **PIa-b** and **PIIa-b** cells depend on the backbone conjugation pattern.

Table 3. Photovoltaic Parameters from Devices of Configuration: ITO/PEDOT:PSS/Polymer:PCBM (1:3 Weight Ratio)/LiF/Al

Code	Active Area (mm^2)	V_{OC} (mV)	I_{SC} (mA/cm^2)	FF (%)	$\eta_{AM1.5}$ (%)
PIa	10.2	900	2.51	54	1.21
PIa	15.3	900	2.44	50.6	1.11
PIb	11	900	3.78	49	1.67
PIb	12.6	900	3.65	53	1.74
PIIa	9	800	4.19	46	1.52
PIIa	13.5	750	4.10	44	1.35
PIIb	8	800	4.45	42	1.50
PIIb	12	800	4.47	40	1.40
PIId	16.2	500	1.44	37.1	0.27
PIId	10.2	600	1.15	36.8	0.25

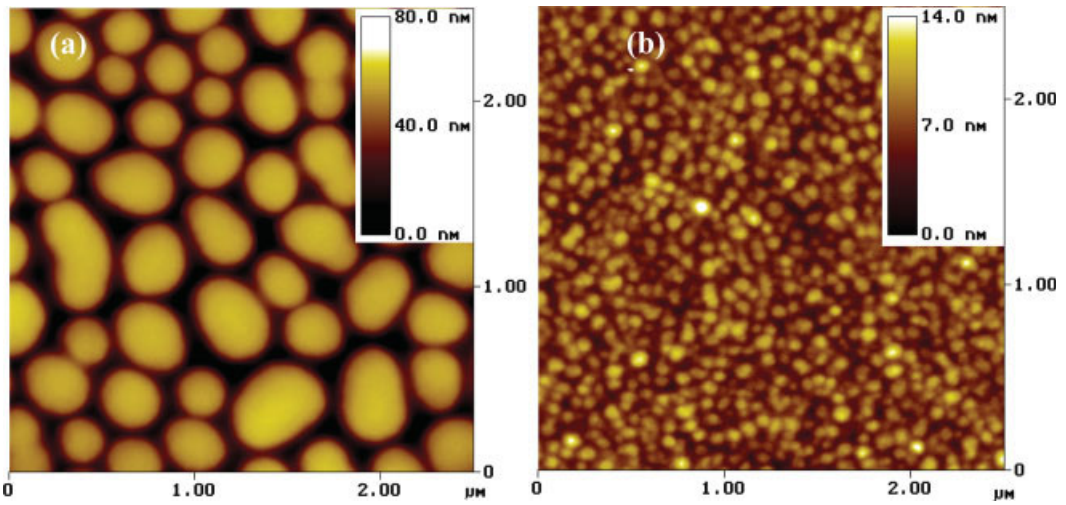

Figure 8. AFM topology of **PIa**:PCBM (a) and **PIb**:PCBM (b) blends. [Color figure can be viewed in the online issue, which is available at www.interscience.wiley.com.]

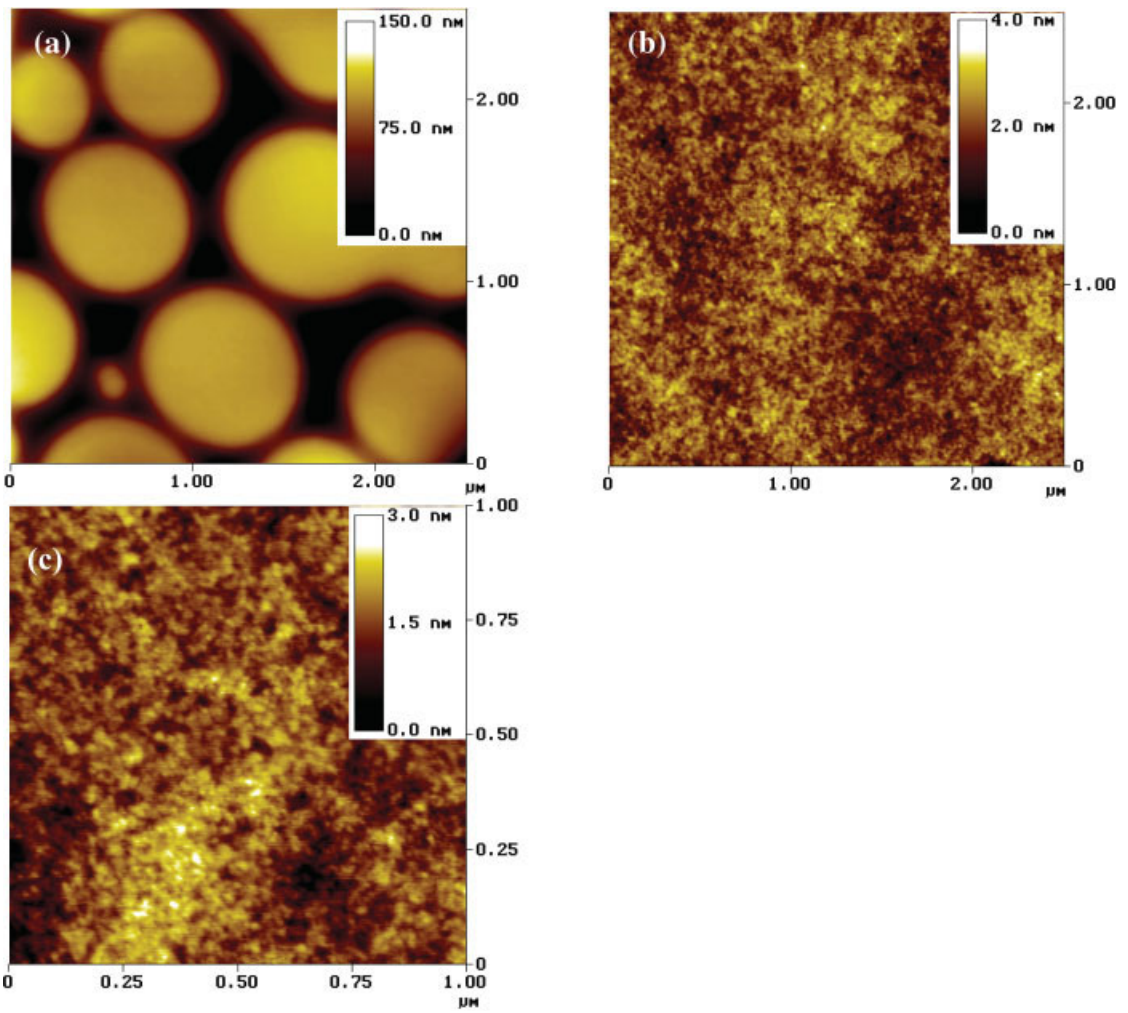

Figure 9. AFM topology of **PIId**:PCBM (a), **PIIa**:PCBM (b), and **PIIb**:PCBM (c) blends. [Color figure can be viewed in the online issue, which is available at www.interscience.wiley.com.]

For instance, the higher number of thiophene units within **PII** systems would explain the lower V_{OC} (800 mA) and higher I_{SC}, compared to **PI** systems.

CONCLUSIONS

High molecular weight, thermostable, and highly soluble thiophene-containing PAE-PAV, **PIa-b**, and **PIIa-b** have been synthesized and characterized. Both classes of compound show identical absorption and emission in solution and in thin film. The band splitting of the thin film absorption is related to various contribution of **H**- and **J**-aggregates. Replacing *linear* octadecyloxy in **PIIc-e** with *bulky* 2-ethylhexyloxy in **PIIa-b** results in an increase of the thin film fluorescence quantum yield from 0 to 3%. The higher the number of thiophene rings within the RU the lower the fluorescence quantum yield. Nonoptimized photovoltaic devices of set up ITO/PEDOT:PSS/polymer:PCBM (1:3 weight ratio)/LiF/Al using **PIa-b** and **PIIa-b** have been designed and studied. V_{OC}'s as high as 900 and 800 mV were obtained for **PIa-b** and **PIIa-b** cells, respectively. Reducing the length and size of side chains from R = 2-*ethylhexyl* in **PIa** to R = *methyl* in **PIb** leads to a significant increase of I_{SC} from ~2.5 to ~3.7 mA and concomitant increase of $\eta_{AM1.5}$ from ~1.2 to ~1.7% due to enhanced donor–acceptor interfacial area as clearly evidenced by AFM pictures of the active layers. Similar change leads to minimal effect in **PII** systems, where approximately the same $\eta_{AM1.5}$ of ~1.50% was achieved from both **PIIa** and **PIIb** cells.

Further structural modifications in the conjugated backbone and optimization of the side groups while maintaining the 1:2 triple bond/*double bond* ratio are presumed to provide new materials with further improved photovoltaic parameters. This aspect is presently under study.

We thank Dr. Eckhard Birckner of the Institute of Physical Chemistry Jena for carrying out the solution fluorescence measurements.

REFERENCES AND NOTES

1. (a) Briehn, C. A.; Kirschbaum, T.; Bäuerle, P. J Org Chem 2000, 65, 352; (b) Wang, Q.; Zakeeruddin, S. M.; Cremer, J.; Bäuerle, P.; Humphry-Baker, R.; Grätzel, M. J Am Chem Soc 2005, 127, 5706; (c) Krämer, J.; Rios-Carrera, I.; Fuhrmann, G.; Musch, C.; Wunderlin, M.; Debaerdemaeker, T.; Mena-Osteritz, E.; Bäuerle, P.; Angew Chem Int Ed Engl 2000, 39, 3481; (d) Roncali, J.; Blanchard, P.; Frère, P. J Mater Chem 2077, 2005, 15; (e) Bäuerle, P. In Electronic Materials: The Oligomeric Approach; Müllen, K.; Wegner, G., Eds.; Wiley-VCH: Weinheim, 1998; pp 105–197.
2. (a) Fachetti, A.; Mushrush, M.; Katz, H. E.; Marks, T. J.; Adv Mater 2003, 15, 33; (b) Facchetti, A.; Letizia, J.; Yoon, M.-H.; Mushrush, M.; Katz, H. E.; Marks, T. J Chem Mater 2004, 16, 4751; (c) Takimiya, K.; Kunugi, Y.; Konda, Y.; Ebata, H.; Toyoshima, Y.; Otsubo, T. J Am Chem Soc 2006, 128, 3044.
3. (a) Roncali, J.; Chem Rev 1992, 92, 711; (b) Loewe, R. S.; Khersonsky, S. M.; McCullough, R. D. Adv Mater 1999, 11, 250; (c) Sheina, E. E.; Liu, J.; Iovu, M. C.; Laird, D. W.; McCullough, R. D. Macromolecules 2004, 37, 3526; (d) Iovu, M. C.; Sheina, E. E.; Gil, R. R.; McCullough, R. C. Macromolecules 2005, 38, 8649.
4. (a) Zen, A.; Pflaum, J.; Hirschmann, S.; Zhuang, W.; Jaiser, F.; Asawapirom, U.; Rabe, J. P.; Scherf, U.; Neher, D. Adv Funct Mater 2004, 14, 757; (b) Schilinsky, P.; Asawapirom, U.; Scherf, U.; Biele, M.; Brabec C. J Chem Mater 2005, 17, 2175.
5. (a) Schwendeman, I.; Hickman, R.; Sonmez, G.; Schottland, P.; Zong, K.; Welsh, D. M.; Reynolds, J. R. Chem Mater 2002, 14, 3118; (b) Sonmez, G.; Shen, C. K. F.; Rubin, Y.; Wudl, F. Angew Chem Int Ed Engl 2004, 43, 1498.
6. (a) McCullough, R. D.; Ewbank, P. E.; Loewe, R. S. J Am Chem Soc 1997, 119, 633; (b) Le Floch, F.; Ho, H. A.; Harding-Lepage, P.; Bedard, M.; Neagu-Plesu, R.; Leclerc, M. Adv Mater 2005, 17, 1251.
7. Villers, D.; Jobin, D.; Soucy, C.; Cossement, D.; Chahine, R.; Breau, L.; Belanger, D. J Electrochem Soc 2003, 150, A747.
8. Tuken, T.; Yazici, B.; Erbil, M. Progr Org Coating 2004, 51, 205.
9. Skotheim, T.; Reynolds, J.; Elsenbaumer, R. Handbook of Conductive Polymers; Marcel Dekker: New York, 1998.
10. (a) Heuer, H. W.; Wehrmann, R.; Kirchmeyer, S. Adv Funct Mater 2002, 12, 89; (b) De Paoli, M. A.; Nogueira, A. F.; Machado, D. A.; Longo, C. Electrochim Acta 2001, 46, 4243; (c) Groenendaal, L. B.; Zotti, G.; Aubert, P. H.; Waybright, S. M.; Reynolds, J. R. Adv Mater 2003, 15, 855.
11. (a) Ong, B. S.; Wu, Y. L.; Liu, P.; Gardner, S. Adv Mater 2005, 17, 1141; (b) Yang, H. C.; Shin, T. J.; Yang, L.; Cho, K.; Ryu, C. Y.; Bao, Z. N. Adv Funct Mater 2005, 15, 671; (c) Garnier, F.; Yassar, A.; Hjlaoui, R.; Horowitz, G.; Deloffre, F.; Servet, B.; Ries, S.; Alnot, P. J Am Chem Soc 1993, 115, 8716.
12. McCulloch, I.; Heeney M.; Bailey C.; Genevicius, K.; MacDonald I.; Shkunov, M.; Sparrowe, D.; Tierney, S.; Wagner, R.; Zhang, W.; Chabinyc, M. L.; Kline, R. J.; McGehee, M. C.; Toney, M. F. Nat Mater 2006, 5, 1.

13. (a) Padinger, F.; Rittberger, R. S.; Sariciftci, N. S. Adv Funct Mater 2003, 13, 85; (b) Hoppe, H.; Sariciftci, N. S. J Mater Chem 2006, 16, 45; (c) Hou, J.; Tan, Z.; Yan, Y.; He, Y.; Yang, C.; Li, Y. J Am Chem Soc 2006, 128, 4911.
14. (a) Brabec, C. J.; Hauch, J A.; Schilinsky, P.; Waldauf, C. MRS Bull 2005, 30, 50; (b) Li, G.; Shrotriya, V.; Huang, J.; Yao, Y.; Moriarty, T.; Emery, K.; Yang, Y. Nat Mater 2005, 4, 864.
15. (a) Ma, W.; Yang, C.; Gong, X.; Lee, K.; Heeger, A. J Adv Funct Mater 2005, 15, 1617; (b) Reyes-Reyes, M.; Kim, K.; Carrolla, D. L. Appl Phys Lett 2005, 87, 083506.
16. (a) Hoppe, H.; Egbe, D. A. M.; Mühlbacher, D.; Sariciftci, N. S. J.; Mater Chem 2004, 14, 3462; (b) Al-Ibrahim, M.; Konkin, A.; Roth, H.-K.; Egbe, D. A. M.; Klemm, E.; Zhokhavets, U.; Gobsch, G.; Sensfuss, S. Thin Solid Films 2005, 474, 201; (c) Egbe, D. A. M.; Nguyen, L. H.; Hoppe, H.; Mühlbacher, D.; Sariciftci, N. S. Macromol Rapid Commun 2005, 26, 1389.
17. (a) Egbe, D. A. M.; Kietzke, T.; Carbonnier, B.; Mühlbacher, D.; Hörhold, H.-H.; Neher, D.; Pakula, T. Macromolecules 2004, 37, 8863; (b) Hoppe, H.; Sariciftci, N. S.; Egbe, D. A. M.; Mühlbacher, D.; Koppe, M. Mol Cryst Liq Cryst 2005, 426, 255; (c) Kietzke, T.; Egbe, D. A. M.; Hörhold, H.-H.; Neher, D. Macromolecules 2006, 39, 4018.
18. (a) Egbe, D. A. M.; Nguyen, L. H.; Carbonnier, B.; Mühlbacher, D.; Sariciftci, N. S. Polymer 2005, 46, 9585; (b) Egbe, D. A. M.; Nguyen, L. H.; Mühlbacher, D.; Hoppe, H.; Schmidtke, K.; Sariciftci, N. S. Thin Solid Films 2006, 511, 486.
19. (a) Leclerc, M.; Faïd, K. Adv Mater 1997, 9, 1087; (b) Drolet, N.; Morin, J.-F.; Leclerc, N.; Wakim, S.; Tao, Y.; Leclerc M. Adv Funct Mater 2005, 15, 1671.
20. Demas, J. N.; Crosby, G. A. J Phys Chem 1971, 75, 991.
21. Teuschel, A. Ph. D. thesis, Friedrich-Schiller-University, Jena, Germany, 1997.
22. (a) Egbe, D. A. M.; Roll, C. P.; Birckner, E.; Grummt, U.-W.; Stockmann, R.; Klemm, E. Macromolecules 2002, 35, 3825; (b) Egbe, D. A. M.; Sell, S.; Ulbricht, C.; Birckner, E.; Grummt, U.-W. Macromol Chem Phys 2004, 205, 2105.
23. (a) Sonogashira, K.; Tohda, Y.; Hagihara, N. Tetrahedron Lett 1975, 50, 4467; (b) Bunz, U. H. F. Chem Rev 2000, 100, 1605.
24. (a) Egbe, D. A. M.; Birckner, E.; Klemm, E. J Polym Sci Part A: Polym Chem 2002, 40, 2670; (b) Egbe, D. A. M.; Carbonnier, B.; Ding, L.; Mühlbacher, D.; Birckner, E.; Pakula, T.; Karasz, F. E.; Grummt, U.-W. Macromolecules 2004, 37, 7451; (c) Egbe, D. A. M.; Carbonnier, B.; Paul, E. L.; Kietzke, T.; Mühlbacher, D.; Birckner, E.; Grummt, U.-W.; Pakula, T.; Neher, D. Macromolecules 2005, 38, 6269.
25. (a) Egbe, D. A. M.; Bader, C.; Nowotny, J.; Günther, W.; Klemm, E. Macromolecules 2003, 36, 5459; (b) Egbe, D. A. M.; Ulbricht, C.; Orgis, T.; Carbonnier, B.; Kietzke, T.; Peip, M.; Metzner, M.; Gericke, M.; Birckner, E.; Pakula, T.; Neher, D.; Grummt, U.-W. Chem Mater 2005, 17, 6022.
26. (a) Bouchard, J.; Belletête, M.; Durocher, G.; Leclerc, M.; Macromolecules 2003, 36, 4624; (b) Tirapattur, S.; Belletête, M.; Drolet, N.; Leclerc, M.; Durocher, G. Chem Phys Lett 2003, 370, 799.
27. (a) Moliton, A.; Hiorns, R. C. Polym Int 2004, 53, 1397; (b) Moliton, A.; Nunzi, J.-M. Polym Int 2006, 55, 583.
28. Gomer, R. J.; Tryson, G. J Chem Phys 1977, 66, 4413.
29. (a) Yamamoto, T.; Takagi, M.; Kizu, K.; Maruyama, T.; Kubota, K.; Kanbara, H.; Kurihara, T.; Kaino, T. J Chem Soc Chem Commun 1983, 797; (b) Yamamoto, T.; Yamada, W.; Takagi, M.; Kizu, K.; Maruyama, T.; Ooba, N.; Tomaru, S.; Kurihara, T.; Kaino, T.; Kubota, K. Macromolecules 1994, 27, 6620.
30. (a) Chen, Z.-K.; Huang, W.; Wang, L. H.; Kang, E. T.; Chen, B. J.; Lee, C. S.; Lee, S. T. Macromolecules 2000, 33, 9015; (b) Yamamoto, T.; Lee, B. L. Macromolecules 2002, 35, 2993.